Hydrodynamic Studies on the Manganese-Stabilizing Protein of Photosystem II†

Igor Z. Zubrzycki,‡,§ Laurie K. Frankel,§ Paul S. Russo,|| and Terry M. Bricker*,§

Department of Biological Sciences, Biochemistry and Molecular Biology Section, and Department of Chemistry, Louisiana State University, Baton Rouge, Louisiana 70803

Received June 22, 1998; Revised Manuscript Received July 28, 1998

ABSTRACT: The solution conformation of the manganese-stabilizing protein of photosystem II was examined by analytical ultracentrifugation. Sedimentation velocity and sedimentation equilibrium studies were performed. These experiments yielded values for $s^0_{20,w}$ of 2.26 S with a diffusion constant, *D*, of 7.7×10^{-7} cm^2 s^{-1}. This *s* value is significantly lower than the apparent *s* value of 2.6 S previously reported [Miyao, M., and Murata, N. (1989) *Biochim. Biophys. Acta 977*, 315−321]. The molecular mass of the protein, 26.531 kDa, was verified by MALDI mass spectrometry. The diffusion coefficient was also determined by dynamic light scattering. The *z*-weighted average of *D* was 6.8×10^{-7} cm^2 s^{-1}. This result was somewhat lower than that observed by analytical ultracentrifugation due to the presence of slowly diffusing components in the sample. A two-component exponential fit of the dynamic light scattering data, however, gave $D = 7.52 \times 10^{-7}$ cm^2 s^{-1} for the major component of the sample, which is in excellent agreement with the value determined by analytical ultracentrifugation. The value of *s**, the apparent sedimentation coefficient, was found to depend on the concentration of the protein and varied about 4% per milligram of protein. This is a feature of proteins which are asymmetric in solution. This asymmetry was examined using both the v-bar and Teller methods. Both methods indicated a significant degree of asymmetry for the manganese-stabilizing protein. Our findings indicate that the prolate ellipsoid model for the manganese-stabilizing protein is elongated in solution, with approximate dimensions of about 12.6 nm × 3.0 nm, yielding an axial ratio of 4.2.

In higher plants and cyanobacteria, at least six intrinsic proteins appear to be required for oxygen evolution by photosystem II (PS II)[1] (*1*−*3*). These are CP 47, CP 43, the D1 protein, the D2 protein, and the α and *β* subunits of cytochrome b_{559}. Insertional inactivation or deletion of the genes for these components results in the complete loss of oxygen evolution activity. Additionally, a number of low molecular mass components appear to be associated with PS II (*4*, *5*), although the functions of these proteins remain obscure. While PS II complexes containing only these components can evolve oxygen, they do so at low rates (about 25−40% of control), are extremely susceptible to photoinactivation, and require high, nonphysiological levels of calcium and chloride for maximal activity (*1, 3*).

In higher plants, three extrinsic proteins, with apparent molecular masses of 33, 24, and 17 kDa, are required for high rates of oxygen evolution at physiological inorganic cofactor concentrations. In cyanobacteria, only the 33 kDa component is present with the functions of the 23 and 17 kDa proteins possibly being provided by cytochrome c_{550} and a 12 kDa protein (*6*). These components apparently interact with intrinsic membrane proteins and possibly with each other to yield fully functional oxygen-evolving complexes. Of the three extrinsic proteins, the 33 kDa component appears to play a central role in the stabilization of the manganese cluster and is essential for efficient and stable oxygen evolution. Because of its pronounced effect on the stability of the manganese cluster at low chloride concentrations, this protein has been termed the manganese-stabilizing protein. Despite a rather large literature examining this component, relatively little is known of its structure or its functional role within the photosystem.

No successful crystallization studies have been reported for the manganese-stabilizing protein, although anecdotal reports suggest that several groups have tried unsuccessfully. Consequently, only low-resolution studies have been performed. These include far-UV CD measurements (*7*, *8*), FTIR studies (*9*), site-specific labeling and mapping experiments (*10*, *11*), and site-directed mutagenesis experiments (*12*, *13*). These investigations have yielded interesting and, in large measure, complementary results (*14*).

† Funding was provided by the generous support of the National Science Foundation to T.M.B. and L.K.F. and, separately, to P.S.R.

* Address correspondence to this author at the Department of Biological Sciences, Biochemistry and Molecular Biology Section, Louisiana State University, Baton Rouge, LA 70803. Telephone: (225) 388-1555. Fax: (225)388-4638. E-mail: BTBRIC@LSUVM.SNCC.LSU.EDU.

‡ Present address: Biochemistry Laboratorium, Institute of Medical Rehabilitation, Technical University of Opole, ul. Dzialkowa 4, 42-154, Opole, Poland.

§ Department of Biological Sciences.

|| Department of Chemistry.

[1] Abbreviations: Bis-Tris, [bis(2-hydroxyethyl)amino]tris(hydroxymethyl)methane; chl, chlorophyll; EDC, 1-ethyl-3-[3-(dimethylamino)propyl]carbodiimide; LiDS, lithium dodecyl sulfate; MALDI, matrix-assisted laser desorption ionization; Mes, 2-(*N*-morpholino)ethanesulfonic acid; PS II, photosystem II; PAGE, polyacrylamide gel electrophoresis; SDS, sodium dodecyl sulfate; TFA, trifluoroacetic acid.

S0006-2960(98)01469-X CCC: $15.00
Published on Web 09/05/1998

Analytical ultracentrifugation is a powerful means for determination of hydrodynamic properties of macromolecules. It allows for direct measurements of sedimentation coefficient, diffusion coefficient, molecular mass, and purity of a protein sample. Analysis of the sedimentation and diffusion coefficients can give insights into the overall shape of a protein. In this study, we have used analytical ultracentrifugation to examine the manganese-stabilizing protein of PS II in solution. Using both sedimentation velocity and sedimentation equilibrium experiments, we have determined the sedimentation and diffusion coefficients of the protein. Additionally, the value of the diffusion coefficient was confirmed by dynamic light scattering measurements, and the molecular mass of the manganese-stabilizing component was confirmed by MALDI mass spectrometry. These studies have allowed us to form hypotheses concerning the overall shape of the molecule. Our findings indicate that the manganese-stabilizing protein, if modeled as a prolate ellipsoid, is elongated in solution, with the approximate dimensions of 12.6 nm × 3.0 nm yielding an axial ratio of 4.2.

MATERIALS AND METHODS

Protein Purification. The manganese-stabilizing protein was purified from store-bought spinach. All procedures for the isolation of this protein were performed at 4 °C. Chloroplasts were isolated as previously described (*15*). PS II membranes were isolated by the procedure of Berthold et al. (*16*) as modified by Ghanotakis and Babcock (*17*). These membranes were suspended to a concentration of 1 mg/mL chl in 1.0 M NaCl, 300 mM sucrose, 10 mM $MgCl_2$, and 50 mM Mes−NaOH, pH 6.0, and incubated for 1 h. The PS II membranes, which were now depleted of the 24 and 17 kDa proteins, were recovered by centrifugation at 36000*g* in a Sorvall SS-34 rotor and resuspended in 1.0 M $CaCl_2$, 300 mM sucrose, 10 mM $MgCl_2$, and 50 mM Mes−NaOH, pH 6.0, which released the manganese-stabilizing protein. After centrifugation at 36000*g* to remove the PS II membranes, the supernatant, which contained the manganese-stabilizing protein, was dialyzed overnight at 4 °C against 10 mM Bis-Tris, pH 6.0. The dialyzed protein solution was centrifuged at 36000*g* to remove a green precipitate and filtered through a 0.22 μm filter, and the protein was concentrated by centrifugal ultrafiltration. The protein was then loaded onto a Bio-Q chromatography column which was equilibrated with 50 mM Bis-Tris, pH 6.0. After washing with several column volumes of this buffer, the manganese-stabilizing protein was eluted with a 0−0.5 M NaCl gradient with the target protein eluting at about 100 mM NaCl. The column fractions containing the manganese-stabilizing protein were pooled and concentrated by centrifugal ultrafiltration.

Analytical Ultracentrifugation. Sedimentation experiments were performed using a Beckman Optima XL-A analytical ultracentrifuge. Sedimentation velocity experiments were performed at 10 and 20 °C at speeds of 70000*g* and 196000*g*. Sample concentrations were 0.1, 0.2, 0.5, 0.7, and 1.4 mg/mL in 20 mM potassium phosphate buffer, pH 6.0, with 200 mM NaCl. Sedimentation equilibrium experiments were performed at sample concentrations of 0.1, 0.2, and 0.5 mg/mL using the same buffer system at 13000*g*, 25000*g*, and 45000*g*. The data were processed using the Origin program supplied by Beckman. The wavelength was adjusted to give an absorbance of about 0.6 for each sample. For each experiment, 20 scans were recorded using XL-A software with the radial increment of 0.05 mm. The delay between scans was equal to 20 min. The analytical acceleration of the rotor was used. All data were transferred from the data acquisition station to a Pentium 120 MHz and were examined using the SVEDBERG program ver. 5.01, which directly fits sedimentation velocity profiles to determine *s* and *D* (*18*, *19*). This approach allows the fitting of experimental velocity data to models derived from an approximation of the Lamm equation, allowing the determination of *s* and *D*. These data were also analyzed with the *g*(*s*) Analysis Program included in the XL-A software.

Only scans with a defined meniscus and plateau were used for further analysis. On average, nine scans were fitted. The accuracy of fitting was checked against molecular weight using the relation:

$$M = sRT/D(1 - \bar{v}\rho) \quad (1)$$

where R is the gas constant, $\bar{v}$ is the partial specific volume, s is the sedimentation coefficient, D is the diffusion coefficient, and ρ is the solvent density. The partial specific volume of the manganese-stabilizing protein was calculated from the derived amino acid composition of the protein using SEDNTERP ver 1.0 (*20*). Solvent density at 20 °C was measured using a Digital Density meter DMA58 (Anton Parr, USA). The viscosity calculation was performed using the data set included in the SEDNTERP program.

MALDI Mass Spectrometry. Mass spectrometry was performed on the manganese-stabilizing protein at the Wistar Protein Microchemistry Laboratory (Philadelphia, PA). Protein samples were diluted to 1−5 pmol/mL with 0.1% TFA, mixed with the matrix (a saturated solution of sinapinic acid), and analyzed with a PerSpective Biosystems Voyager Biospectrometry Workstation. Two internal mass standards, carbonic anhydrase (29.024 kDa) and bovine serum albumin (66.431 kDa), were used for instrument calibration. MALDI mass spectra were analyzed using the GPMAW Program (Lighthouse Data, Denmark).

Dynamic Light Scattering. All samples were filtered through 0.22 μm filters and placed in a cuvette inside a custom, temperature-regulated DLS instrument. A Spectra-Physics Millennia II laser operating at 532 nm was used as the light source. The experiments were performed at sample concentrations of 0.3 mg/mL and 0.7 mg/mL at a scattering angle of 90° and a temperature of 20 °C. All data were collected and processed using the ALV-5000 digital autocorrelator (ALV−Langen, Germany), using its associated software and custom-written software. As the solutions were not completely free from particulate matter, and as extensive attempts to remove "dust" can result in loss of protein, the correlation functions were collected in 10 or 20 s bursts. This corresponds to several hundred thousand decay times. The "multi-run" feature of the autocorrelator was set to inspect the intensity trace of each short run and automatically reject poor runs until 10 acceptable short runs (100 or 200 s usable acquisition time) were obtained. The entire trace, not the instantaneous intensity which contains the useful information, was used by the correlator software to decide whether a given short run should be retained. Each short run was also

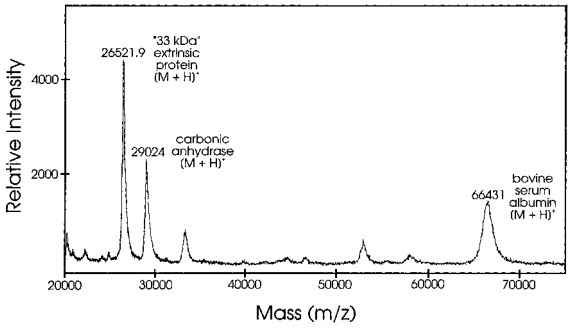

FIGURE 1: MALDI mass spectrum of the manganese-stabilizing protein of PS II and internal molecular mass standards. The $(M + H)^+$ ions for the manganese-stabilizing protein and the internal standards carbonic anhydrase and bovine serum albumin are labeled.

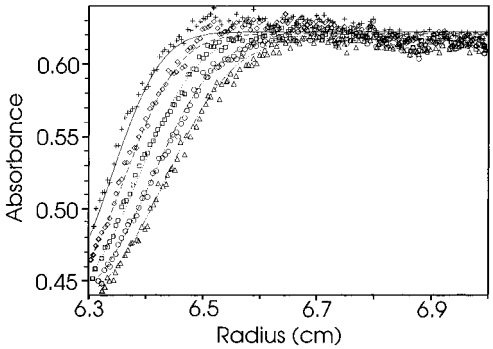

FIGURE 2: Sedimentation velocity analysis of manganese-stabilizing protein of photosystem II. The sample concentration was 0.2 mg/mL in 20 mM potassium phosphate buffer and 200 mM NaCl, pH 7. The sample was centrifuged at 196000*g* at 20 °C. Five consecutive scans, collected at the time interval of 10 min, are best fit to a conventional cell, modified Fujita−MacCosham function 1 species using the SVEDBERG program (*18*). The data were truncated at the end of the first, low abundance, slowly sedimenting plateau (radius = 6.3 cm) for this analysis.

inspected visually and analyzed by the method of cumulants (*21*) before computing the average correlation function.

RESULTS AND DISCUSSION

Figure 1 shows a typical mass spectrum of the spinach manganese-stabilizing protein as obtained by MALDI mass spectrometry. Internal molecular mass standards were added to the sample of the manganese-stabilizing protein and were used to calibrate the mass spectrometer. The apparent mass of the manganese-stabilizing protein was 26.515 kDa (s = 0.016 kDa, $n = 3$). The calculated molecular mass of this protein, which is derived from the predicted amino acid sequence, is 26.531 kDa. Comparison of the predicted mass of the manganese-stabilizing protein with the mass measured by MALDI mass spectrometry indicates an error of 0.06%, which is within the error envelope of this instrument. These findings indicate that the manganese-stabilizing protein does not appear to be posttranslationally modified, at least at a level which could be identified with this instrumentation. This allows the use of the derived amino acid sequence of the protein for the determination of its partial specific volume.

The sedimentation velocity studies were performed at the following conditions: sample concentrations, 0.1, 0.2, 0.5, 0.7, 1.0, and 1.4 mg/mL; temperatures, 10 and 20 °C; 70000*g* and 195000*g*. For experiments performed at 20 °C, 195000*g*, and sample concentrations of 0.1 and 0.2 mg/mL, two discrete boundaries were observed. The first, slowly sedimenting component was estimated to be present at 2.5−5% of the concentration of the second, more rapidly sedimenting component based on absorbance measurements. It should be noted that LiDS−PAGE of the protein sample confirmed the presence of a low molecular mass component with a molecular mass of 5−10 kDa with an estimated abundance of about 5% based on Coomassie Blue staining (data not shown). The slower sedimenting component was not observed at higher concentrations of protein. All data sets were analyzed using the SVEDBERG program. The data sets with two visible boundaries (0.1 and 0.2 mg/mL protein) were truncated at the end of the first plateau and analyzed using the conventional cell, modified Fujita−MacCosham function 1 species (*19*) (Figure 2). This analysis yielded s values of 2.26 and 2.24 S with a confidence interval of 95%, and D values of 7.70×10^{-7} and 7.67×10^{-7} cm^2 s^{-1} for the 0.1 and 0.2 mg/mL protein samples, respectively. This analysis was verified by using eq 1 shown under Materials and Methods. The fitted values of s and D for 0.1 and 0.2 mg/mL yielded a calculated molecular mass for the manganese-stabilizing protein of 26.65 and 26.52 kDa, respectively, using $\upsilon = 0.7317$ mL/g. These values are in excellent agreement with the actual molecular mass of 26.531 kDa as determined by analysis of the derived amino acid sequence and as experimentally determined by MALDI mass spectrometry (Figure 1). The data sets obtained at the concentrations of 0.5, 0.7, 1.0, and 1.4 mg/mL were also analyzed using the SVEDBERG program; however, the conventional cell Fujita−MacCosham function 2 species option was selected (*19*). This analysis yielded sedimentation coefficients for the major component of 2.22, 2.19, 2.16, and 2.14 S, respectively. To verify the fitted s values, the data sets obtained for sample concentrations of 0.1 and 0.2 mg/mL protein were subjected to $g(s)$ analysis which yielded sedimentation coefficients of 2.25 and 2.20 S, respectively. These values are in good agreement with the values obtained from the SVEDBERG program. Thus, analysis of the sedimentation velocity data by two independent methods [direct fitting and $g(s)$ analysis] yielded very similar s values.

Miyao and Murata (*22*) have also determined a sedimentation coefficient for the manganese-stabilizing protein. They reported an *apparent s* value of 2.6 S, which is considerably larger than our $s^0_{20,w}$ value of 2.26 S. It should be noted that these authors examined neither the effects of protein concentration on s nor the effects of varying the angular velocity or temperature on this parameter. Their experiments were also performed at low ionic strength (10 mM Mes−NaOH, pH 6.5). In some experiments, they examined the effect of the addition of 10 mM NaCl or 5 mM $CaCl_2$. It is unclear, at this time, why these authors obtained a different s value than that reported in this paper.

As noted above, the sedimentation velocity experiments and LiDS−PAGE analysis indicated the presence of a minor, low molecular mass component in the protein samples used in these experiments. This was confirmed by sedimentation equilibrium experiments, a typical result of which is shown in Figure 3. When these data were fitted to a single sedimenting species, nonrandom residuals were observed. When the data were fitted to a two-component model, however, random residuals were observed. This strongly

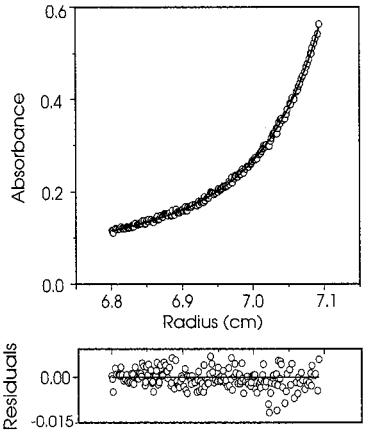

FIGURE 3: Analysis of the sedimentation equilibrium data obtained for the manganese-stabilizing protein. The initial sample concentration was 0.2 mg/mL and centrifuged at 45000*g* at 20 °C. The concentration distribution changes were recorded at 276 nm using 20 averages and the radial step of 0.001 mm. The plot was fitted using the ORIGIN program with an ideal-2 species model. Apparent masses for the two species were 4.87 (±0.98) kDa and 28.04 (±2.36) kDa.

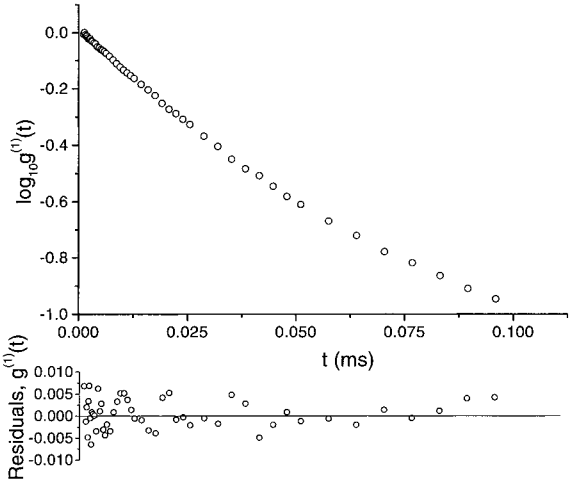

FIGURE 4: Semilogarithmic plot of the normalized first-order autocorrelation function $g^1(t)$ for the manganese-stabilizing protein at 0.7 mg/mL obtained by dynamic light scattering. Residuals are shown for a two-component exponential fit to $g^1(t)$.

suggested the presence of two sedimenting species. The apparent molecular mass of the major component was calculated to be 28.04 kDa (±2.36 kDa) while that of the minor component was 4.77 kDa (±0.98 kDa). These results are fully consistent with the results obtained from the sedimentation velocity experiments and LiDS−PAGE analysis.

Dynamic light scattering was used to verify the diffusion coefficient of the manganese-stabilizing protein. The correlation functions from the dynamic light scattering measurements were not single-exponential decays, as evidenced by smooth curvature in the semilogarithmic plots of the normalized correlation function against lag time (Figure 4). Unlike sedimentation velocity, which can physically separate inhomogeneous molecules, in dynamic light scattering experiments individual decay components must be resolved. Several Laplace inversion algorithms are available for this purpose (*23*, *24*). The program CONTIN (*24*) produces several distributions of the diffusion coefficient, $g(D)$, that are compatible with the measured correlation function. It then applies statistical tests to select the smoothest distribution consistent with the data. For either concentration, the chosen distribution consisted of a single, broad peak. Rather than obtain the average over the entire distribution from this peak, which usually suffers from an ill-defined amount of computational broadening, simple cumulants analysis was performed on the averaged correlation functions, which were essentially identical at 0.3 and 0.7 mg/mL. The cumulant algorithm (*21*) yields the *z*-average of the diffusion coefficient, thus heavily favoring any high mass components that may be present. Less importance is assigned to small, rapidly diffusing molecules. Using this method, the average diffusion coefficient obtained for the two concentrations was 6.70×10^{-7} cm^2 s^{-1}. Although the measurements at the different protein concentrations agreed to within 0.01×10^{-7} cm^2 s^{-1}, indicating good precision and negligible concentration effect, the true accuracy of the result is about ±3% when systematic errors are considered. The −13% difference between the diffusion coefficient from dynamic light scattering with cumulants analysis and that from sedimentation is significant. The difference probably reflects the great sensitivity to large mass particles within the sample of dynamic light scattering with cumulants analysis.

To gain a better insight to the inhomogeneous nature of the samples, and recognizing that data analysis in terms of discrete exponential decays analysis will sometimes resolve decay components that CONTIN does not, we applied a two-component exponential fit to the dynamic light scattering data. For the two protein concentrations, 10−20% of the signal was associated with a weak, slowly diffusing component corresponding to a diffusion coefficient of 7.0×10^{-8} cm^2 s^{-1}. This represents either protein aggregates or high molecular mass nonprotein material (such as leached chromatography bed material or DNA). About 80−90% of the scattering signal was associated with a faster diffusing component exhibiting a diffusion coefficient of 7.52×10^{-7} cm^2 s^{-1}. As with the cumulant result, this value is more precise ($\pm 0.02 \times 10^{-7}$ cm^2 s^{-1} for the two concentrations) than accurate (about 3%) when potential systematic errors are considered. The diffusion coefficient obtained from sedimentation velocity (7.7×10^{-7} cm^2 s^{-1}) now agrees with the dynamic light scattering result to within its estimated accuracy.

Thus, the sample of the manganese-stabilizing protein appeared to contain three components. In the sedimentation velocity (at 0.1 and 0.2 mg/mL protein) and equilibrium experiments, both rapidly sedimenting and slowly sedimenting components were observed. The rapidly sedimenting component corresponded to the manganese-stabilizing protein, which had an abundance of about 95%, while the slowly sedimenting component had an apparent molecular mass of about 5 kDa and an abundance of about 5%. These results were confirmed by LiDS−PAGE. In the dynamic light scattering experiments, both rapidly diffusing and slowly diffusing components were observed. The rapidly diffusing component corresponded to the manganese-stabilizing protein while the slowly diffusing component remains unidentified. We hypothesize that this component may be large protein aggregates, polymeric chromatography bed material which has leached into the sample, or possibly DNA. It is emphasized that while the amount of this material is very low (about 10000× lower than the amount of monomeric protein), light scattering is very sensitive to its presence while

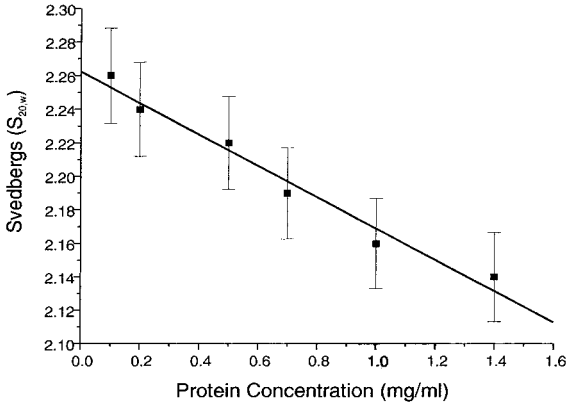

FIGURE 5: Concentration dependence of the apparent sedimentation coefficient *s** of the manganese-stabilizing protein. The solid line represents a linear regression fit of the data. The $s^0_{20,w}$ was determined by extrapolation to zero protein concentration, yielding the value 2.26 S. Error bars indicate ±1.0 SE.

sedimentation experiments are not. Additionally, it is not surprising that the 5 kDa component observed in the sedimentation experiments and LiDS−PAGE was not observed in the dynamic light scattering experiments since this method is highly mass-dependent.

The *s* values obtained from the sedimentation velocity experiments were corrected for concentration effects and extrapolated to zero protein concentration as shown in Figure 5. This yielded an $s^0_{20,w}$ value of 2.26 S for the manganese-stabilizing protein. The concentration dependence of *s*, which is shown in Figure 5, is a feature of asymmetric molecules (*25*, *26*). Typically, one observes about a 1% per mg/mL protein decrease in *s* values for spherical molecules with increasing protein concentration. Asymmetric molecules exhibit larger changes. Our experiments indicated a 4% change in the observed *s* values per mg/mL protein. This result suggests that the manganese-stabilizing protein is asymmetric in solution. To investigate this possibility, these data were analyzed by the SEDNTERP program using both the v-bar and the Teller methods (*27*). These methods yield estimates of the degree of asymmetry of sedimenting particles and allow for the modeling of the manganese-stabilizing protein as either prolate or oblate ellipsoids of revolution. Additionally, these methods allow an estimation of the degree of hydration for the modeled molecules. The values for R_o and R_p (radius of an equivalent anhydrous sphere using the v-bar and Teller methods, respectively), f_o and f_p (minimal frictional coefficient for the v-bar and Teller methods, respectively), and *f* (experimental frictional coefficient) as well as υ were calculated. These treatments yielded the following parameters for the v-bar and Teller methods: v-bar method (prolate model), axial *a*/*b* ratio 4.4, $2a = 12.3$ nm, $2b = 2.8$ nm, and hydration expansion = 16.8%; Teller method (prolate model), axial *a*/*b* ratio 4.2, $2a = 12.1$ nm, $2b = 2.9$ nm, and hydration expansion = 16.2%; v-bar method (oblate model), axial *a*/*b* ratio 4.7, $2a = 7.7$ nm, $2b = 1.7$ nm, and hydration expansion = 16.8%; Teller method (oblate model), axial *a*/*b* ratio 4.5, $2a = 7.7$ nm, $2b = 1.7$ nm, and hydration expansion = 16.2%. Representative prolate and oblate ellipsoids of revolution (v-bar method) are shown in Figure 6A and Figure 6B, respectively. It should be pointed out that it is impossible to differentiate between these two models (prolate vs oblate) based on

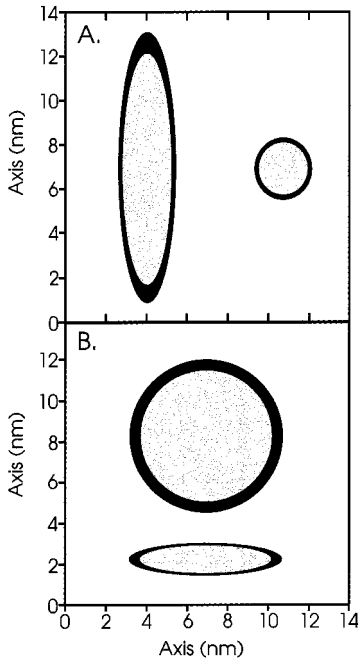

FIGURE 6: Ellipsoids of revolution models obtained from sedimentation velocity parameters. (A) Hydrated prolate model, v-bar method, $a/b = 4.4$ nm, $2a = 12.3$ nm, $2b = 2.8$ nm, hydration expansion = 16.8%; (B) hydrated oblate model, v-bar method, $a/b = 4.7$ nm, $2a = 7.7$ nm, $2b = 1.65$ nm, hydration expansion = 16.8%. Anhydrous versions are shown in gray. Expansion due to hydration is shown in black. Both models were constructed using the SEDNTERP program.

sedimentation data alone. Proteins are usually modeled using the prolate representation, but there is no *a priori* reason for exclusion of the oblate form.

Caution should be exercised when evaluating the above asymmetry results critically. Many assumptions are implicit in the equations used to model the overall shape and degree of hydration of proteins by the use of sedimentation data (*28*−*30*). We have sought to minimize these problems by measuring experimentally as many parameters as possible, including $s^0_{20,w}$, *D* (by sedimentation and dynamic light scattering), the mass of the manganese-stabilizing protein, the density of the solvent, etc., but it remains difficult to separate shape effects from hydration. It is stressed that the central result, the anisotropic shape of the manganese-stabilizing protein, can be obtained without these programs, simply by combining the mass and diffusion data as was formerly common practice. These findings should be interpreted as providing a preliminary evaluation of the asymmetry and degree of hydration until other, higher resolution, information is available.

Other investigators have noted unusual properties exhibited by the manganese-stabilizing protein in solution. The mass of this component is significantly overestimated by SDS−PAGE which yields a mass estimate 25% higher than that deduced by nucleotide sequencing of the *psb*O gene (*31*) or as determined by MALDI mass spectrometry (this work). Proteins which exhibit reduced SDS binding migrate anomalously slowly, yielding artifactually high molecular weight estimates (*32*). It is unclear, however, if this is the case for the manganese-stabilizing protein. Analytical gel filtration studies have indicated a molecular mass of 37−42 kDa for this protein (*33*), which overestimates its actual mass by 40−

60%. This result would be expected of a protein with an extended structure and a high axial ratio. The analytical gel filtration experiments are, thus, consistent with the results presented in this paper.

Our study indicates that the manganese-stabilizing protein has an extended structure in solution. Indeed, the long axis of the protein (in the prolate model) would appear to be capable of spanning nearly the entire PS II core complex monomer, which may have dimensions of 13.6 nm × 9.7 nm (*34*). While this may be the case, it is also quite possible that the manganese-stabilizing protein undergoes substantial conformational changes upon binding to the intrinsic components of the photosystem. This could lead to a significantly more compact structure for the protein when it is associated with PS II. FTIR evidence may support this hypothesis. In an isotope-editing study, Barry and coworkers have determined that there is a large increase in the strength of hydrogen bonding when the manganese-stabilizing protein associates with the photosystem (*9*). They have interpreted this alteration to conformational changes induced by binding of the protein to PS II. Additionally, Enami et al. (*35*) have recently reported that the generation of intramolecular cross-links in the manganese-stabilizing protein with EDC results in the loss of the protein's ability to reconstitute oxygen evolution. They proposed that intramolecular cross-linking leads to the loss of structural flexibility of the molecule, which prevented the manganese-stabilizing protein from undergoing normal conformational changes upon binding to PS II.

In earlier studies, we have presented circular dichroism results which indicate that the spinach manganese-stabilizing protein contains a high proportion of β-sheet structure (33%) and a small amount of α-helical structure (7%) in solution (*7*). This result was recently confirmed (*8*). We have presented a simplistic folding model of the manganese-stabilizing protein which hypothesizes that the β-sheet domains are organized to form four antiparallel β-sheet bundles (*14*) which are separated by random/turn secondary structural elements. This model appears to be very consistent with both site-specific labeling and site-directed mutagenesis studies [for a review, see (*14*)]. Portions of the protein which can be labeled only when the protein is free in solution cluster with amino acid residues whose alteration leads to loss of PS II binding and/or loss of PS II function. These residues all lie in domains which appear to be associated with the intrinsic PS II components. Residues which can be modified when the manganese-stabilizing protein is associated with PS II cluster in domains which are associated with the bulk solvent. Any conformational changes occurring to the manganese-stabilizing protein upon binding to PS II would appear to preserve this vectoral orientation of PS II-associated verses bulk solvent-associated domains.

REFERENCES

1. Murata, N., Mijao, M., Omata, T., Matsunami, H., and Kuwabara, T. (1984) *Biochim. Biophys. Acta 765*, 363−369.
2. Burnap, R. L., and Sherman, L. A. (1991) *Biochemistry 30*, 440−446.
3. Bricker, T. M. (1992) *Biochemistry 31*, 4623−4628.
4. Ikeuchi, M., Koike, H., and Inoue, Y. (1989) *FEBS Lett. 242*, 263−269.
5. Bricker, T. M., and Ghanotakis, D. (1996) in *Oxygenic Photosynthesis: The Light Reactions* (Yocum, C. F., and Ort, D. R., Eds.) Vol. 4, pp 113−136, Kluwer Academic Press, Dordrecht.
6. Shen, J.-R., and Inoue, Y. (1993) *Biochemistry 32*, 1825−1832.
7. Xu, Q., Nelson, J., and Bricker, T. M. (1994) *Biochim. Biophys. Acta 1188*, 427−431.
8. Shutova, T., Irrgang, K.-D., Shubin, V., Klimov, V. V., and Renger, G. (1997) *Biochemistry 36*, 6350−6358.
9. Hutchison, R., Betts, S. D., Yocum, C. F., and Barry, B. A. (1998) *Biochemistry 37*, 5643−5653.
10. Frankel, L. K., and Bricker, T. M. (1995) *Biochemistry 34*, 7492−7497.
11. Odom, W. R., and Bricker, T. M. (1992) *Biochemistry 31*, 5616−5620.
12. Betts, S. D., Ross, J. R., Pichersky, E., and Yocum, C. F. (1996) *Biochemistry 35*, 6302−6307.
13. Betts, S. D., Ross, J. R., Pichersky, E., and Yocum, C. F. (1997) *Biochemistry 36*, 4047−4053.
14. Bricker, T. M., and Frankel, L. K. (1998) *Photosynth. Res. 56*, 157−173.
15. Bricker, T. M., Pakrasi, H. B., and Sherman, L. A. (1985) *Biochim. Biophys. Acta 237*, 170−176.
16. Berthold, D. A., Babcock, G. T., and Yocum, C. F. (1981) *FEBS Lett. 134*, 231−234.
17. Ghanotakis, D. F., and Babcock, G. T. (1983) *FEBS Lett. 153*, 231−234.
18. Philo, J. (1994) in *Modern Analytical Ultracentrifugation* (Schuster, T. M., and Laue, T. M., Eds.) pp 156−170, Birkhauser, Boston.
19. Philo, J. (1997) *Biophys. J. 72*, 435−444.
20. Hayes, D. B., Laue, T., and Philo, J. (1997) Copyright 1995−1997, the University of New Hampshire.
21. Koppel, D. E. (1972) *J. Chem. Phys. 57*, 4814.
22. Miyao, M., and Murata, N. (1989) *Biochim. Biophys. Acta 977*, 315−321.
23. Bott, S. (1983) in *Measurement of Suspended Particles by Quasielastic Light Scattering* (Dahneke, B. E., Ed.) pp 130−157, Wiley, New York.
24. Provencher, S. W. (1982) *Comput. Phys. 27*, 229−242.
25. Creeth, J. M., and Knight, C. G. (1965) *Biochim. Biophys. Acta 102*, 549.
26. Rowe, A. J. (1977) *Biopolymers 16*, 2595−2611.
27. Teller (1973) *Methods Enzymol. 28*, 346−441.
28. Cassasa, E. F., and Eisenberg, H. (1964) *Adv. Protein Chem. 19*, 287.
29. Kirschner, M. W., and Schachman, H. K. (1971) *Biochemistry 10*, 1900.
30. de la Torre, J. G. (1992) in *Analytical Ultracentrifugation in Biochemistry and Polymer Science* (Harding, S., and Rowe, A., Eds.) pp 333−345, Royal Society of Chemistry, London.
31. Tyagi, A., Hermans, J., Steppuhn, J., Jansson, C., Vater, F., and Herrmann, R. G. (1987) *EMBO J. 207*, 288−293.
32. Hames, B. D. (1981) in *Gel Electrophoresis of Proteins: A practical approach* (Hames, B. D., and Rickwood, D., Eds.) pp 1−91, IRL Press Limited, Oxford and Washington, D.C.
33. Betts, S. D., Ross, J. R., Pichersky, E., and Yocum, C. F. (1995) in *Photosynthesis: From Light to Biosphere* (Mathis, P., Ed.) Vol. II, pp 385−388, Kluwer Academic Press, Dordrecht.
34. Hasler, L., Ghanotakis, D., Fedtke, B., Spyridaki, A., Miller, M., Muller, S. A., Engle, A., and Tsotis, G. (1997) *J. Struct. Biol. 119*, 273−283.
35. Enami, I., Kamo, M., Ohta, H., Takahashi, S., Miura, T., Kusayanagi, M., Tanabe, S., Kamei, A., Motoki, A., Hirano, M., Tomo, T., and Satoh, K. (1998) *J. Biol. Chem. 273*, 4629−4634.

BI981469Y